Far-field plasma properties of low-power iodine-fed Hall thruster propulsion system

Francesco M Bianchi, Alfio E Vinci, Laurent Garrigues

Far-field plasma properties of low-power iodine-fed Hall thruster propulsion system

IEPC-2025-281

Presented at the 39th International Electric Propulsion Conference, Imperial College London, London, United Kingdom
14-19 September 2025

Francesco M. Bianchi* and Alfio E. Vinci†
ThrustMe, Verriéres-le-Buisson, 91370, France

Laurent Garrigues‡
LAPLACE, Universit´e de Toulouse, CNRS, INPT, UPS, 31062, Toulouse, France

The properties of the plume generated by an iodine-fed Hall thruster are measured and presented. Current density and ion energy are analyzed. The development of a combined Wien filter and Retarding Potential Analyzer probe is presented, including Particle-In-Cell simulations and experimental results. Preliminary results show the probe design is capable of discriminating ions based on their velocity and energy. Finally, a non-negligible quantity of ionized molecules is found in the plume.

I. Introduction

A subject of great interest within the electric propulsion community is the utilization of iodine as a cheaper and more readily available alternative to xenon. Iodine provides performance comparable to that of xenon while being characterized by higher storage density and a significant fraction of the cost. Iodine-fed electric propulsion has been demonstrated by ThrustMe [1], with currently more than 100 iodine-fed gridded ion engines operating in orbit. However, at higher power regimes, Hall thrusters (HTs) are often the preferred choice, thanks to their high thrust-to-power ratio. In particular, large constellations such as Starlink have been known to employ krypton-fed and argon-fed HT systems. Iodine-fed HTs have been tested in laboratory conditions at various power levels [2–4]. ThrustMe is aiming for an in-orbit demonstration of an iodine-fed HT by 2026 [5].

One of the main questions regarding iodine-fed HTs is related to their plasma chemistry. Iodine, unlike xenon, is present in both atomic (I) and molecular form (I_2). This is particularly interesting, given the effect the presence of ionized molecules (I_2^+) could have on the thruster's performance. Finally, given the electronegative nature of iodine, negative ions (I^-) might be found in the discharge, further complicating its characteristics. These phenomena have been tackled by both numerical studies [6] and experimental works, such as Szabo et al. [2], who used a Wien filter (also known as an $E \times B$ probe) to measure the composition of the ion beam.

This work investigates the plasma properties of the plume produced by JPT150, the low-power iodine-fed HT developed at ThrustMe, and the development of an energy analyzer and Wien filter combined probe.

*PhD Candidate, ThrustMe (associated with LAPLACE Université de Toulouse), francesco.bianchi@thrustme.fr
†Plasma Physicist, ThrustMe, alfio.emanuele.vinci@thrustme.fr
‡Director of Research at CNRS, LAPLACE, laurent.garrigues@laplace.univ-tlse.fr

II. Methodology

A. Thruster and vacuum facility

The JPT150 is an iodine-fed Hall thruster, designed to operate at a discharge power of 150 W. It makes use of an iodine-fed plasma bridge cathode, unlike previous prototypes which relied on xenon-fed neutralizers [2]. All tests were conducted inside of the TM2 vacuum facility, an iodine-compatible chamber with a diameter of 1 m and a length of 2m. It is capable of achieving backpressure in the order of $3 \cdot 10^{-5}$ hPa during thruster operation.

Plasma probes are moved by a rotation stage whose pivot point is aligned with the exit plane of the thruster. This allows measurements along a semicircle around the thruster. The rotation resolution reads about 0.1 deg. Probe alignment is performed using a cross laser pendulum.

B. Current density and ion energy probe

Ion energy distribution is analyzed with a single grid Retarding Potential Analyzer (RPA) probe, part of the combined RPA and Wien filter probe. Said RPA device is also utilized to measure ion current density by grounding its collector and biasing the grid to repel electrons. The grid's geometrical transparency is 22%. The probe is mounted on the rotating arm and is placed approximately at about 20 thruster radii from the thruster's exit plane. Wien filter measurements are conducted at the same distance from the thruster and along the thruster's centerline.

C. Development of an RPA and Wien filter combined probe

1. Operating principle

A Wien filter is a device capable of measuring the velocity distribution function of an ion beam. Given that the velocity of an ion accelerated by an electrostatic thruster is dependent on its charge to mass ratio Zq/m_{ion}, where Z is the ionization number, and given that the ion species found in the plume (I^+,I^{2+},I_2^+) have different charge to mass ratios, a Wien filter can be used to measure the beam composition. The Wien filter operates by applying an electric field and a magnetic field and both perpendicular to the ion beam that enters the probe. These fields are perpendicular to each other and to the direction of ions, as shown in Fig.1. An ion moving across the probe is thus subject to the Lorentz force, defined as:

$$\vec{F} = Zq(\vec{E} + \vec{v}_{ion} \times \vec{B}) \tag{1}$$

The two components of the Lorentz force act along the same axis but in opposite directions. For a given electric field and magnetic field intensity, ions with a velocity $v = E/B$ will be subjected to equal opposing forces and thus proceed unperturbed to the collector. Faster and slower ions will be deviated by magnetic and electric fields respectively. By sweeping the intensity of the electric field E, it is possible to measure the ion velocity distribution function (IVDF).

The probe presented in this work is a combined RPA and Wien filter probe, schematically shown in Fig.1. By adding an RPA in front of the Wien filter, it is possible to discriminate ions based on both velocity and energy, and thus obtain species-specific ion energy distribution functions (IEDFs). After being filtered by a single grid RPA, ions pass through an orifice in the RPA collector and enter the $E \times B$ section.

2. Probe design

The probe is entirely designed within ThrustMe. A compact form factor is preferred, so that the probe can be easily moved around the thruster by a rotating arm. This provides the possibility to store the probe away from the ion beam when no measure is taking place, avoiding unnecessary damage due to ion bombardment. Furthermore, it allows off-axis measurements, particularly interesting given the large fraction of I_2^+ Szabo et al. measured in the off-axis region of the beam[7]. The RPA is composed of a molybdenum grid and collector. Molybdenum was chosen for its resistance to iodine vapor and for its low secondary electron emission yield. A 0.15 mm orifice in the RPA collector allows a beam of ions to enter the Wien filter section. The orifice size was chosen so to ensure that the potential at the center of the orifice, which is the effective retarding potential, would not deviate largely from that of the RPA collector, while still letting enough ions reach the Wien filter collector.

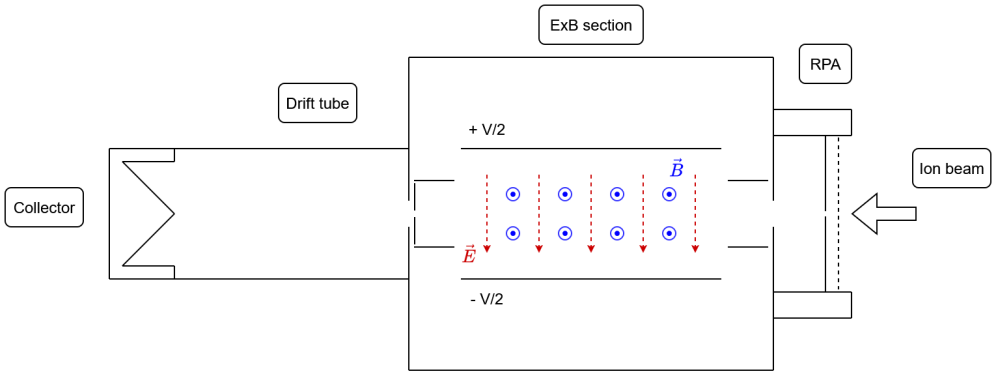

Figure 1: Diagram of the RPA Wien filter combined probe. Not in scale.

Permanent magnets are used to generate the magnetic field. The outer components of the Wien filter are constructed out of AISI 1020 steel due to its ferromagnetic properties. These components help direct the magnetic flux, ensuring that the magnetic field at the center of the probe is homogeneous and aligned. The intensity of the magnetic field along the centerline of the probe reaches 0.18 T. Two molybdenum electrodes produce the desired electric field. They are biased in symmetrical fashion, allowing the centerline of the probe to have a potential equal to facility ground. At the inlet and exit of the $E \times B$ section two collimator tubes are placed. Initial designs involved aluminum collimator tubes that were too long and would partially shield the ion beam from the electric field, allowing the magnetic field to introduce an unwanted deviation. At the outlet of the Wien filter section, a molybdenum disc with a 0.5 mm orifice improves the probe's resolution by allowing only the less perturbed ions to reach the collector. A conical shape is chosen for the collector of the Wien filter in order to reduce the impact of secondary electron emission. The collector is placed at the end of a drift tube to improve the probe's resolution. During measures, the collector is biased to -5 V relative to facility ground in order the repel slow electrons possibly present inside of the probe. All structural elements of the probe are grounded. The Wien filter section is about 40 mm in length, with the electrodes sitting 10 mm from each other. The drift tube length is around 40 mm.

3. Numerical simulation of Wien filter

In order to aid the design of the probe, a series of numerical simulations are conducted. The open source X11 Object-Oriented Particle In Cell (XOOPIC) code is used [8]. The simulation uses a 2D slab domain. The magnetic field is calculated by a COMSOL simulation of the ferromagnetic circuit and is used as an input of the XOOPIC simulation. The simulation involves electrons, single charged atoms (I^+), single charged molecules (I_2^+) and double charged atoms (I^{2+}). The species are injected into the domain from the boundary in front of the RPA grid. The total ion current flux is 3 A/m^2, as measured experimentally at 23 channel lengths from the exit plane. The incoming ion current flux is subdivided among the three ion species according to a 0.8/0.15/0.05 subdivision for $I^+/I_2^+/I^{2+}$ respectively, based the data by Szabo et al.[7] and the results of previous numerical work[6]. The incoming electron flux satisfies quasi-neutrality conditions. All ion species enter the domain with 250 eV energy along the probe axis. Ion are assumed to have a thermal velocity (in addition to their drift velocity) and their temperature is assumed to be 600 K.

The simulation timestep is 10^{-10} s . The mesh is composed of square cells 0.1 mm in size. Super particle weights are $5 \cdot 10^5$, $5 \cdot 10^5$,10^5 and 10^4 for electrons, I^+, I_2^+ and I^{2+} respectively.

Simulations show the Wien filter adequately deviating the ion beams. However, due to their thermal velocity, ions spread significantly once inside of the filter, as visible in Fig.2. This effectively reduces the ability of the probe to resolve the three species individually, as their beams overlap significantly as the electric field across the Wien filter is swept. Figure 2 shows an example snapshot of a simulation case in which the Wien filter voltage allows for single charged ions to reach the collector while deviating ionized molecules and doubly charged ions.

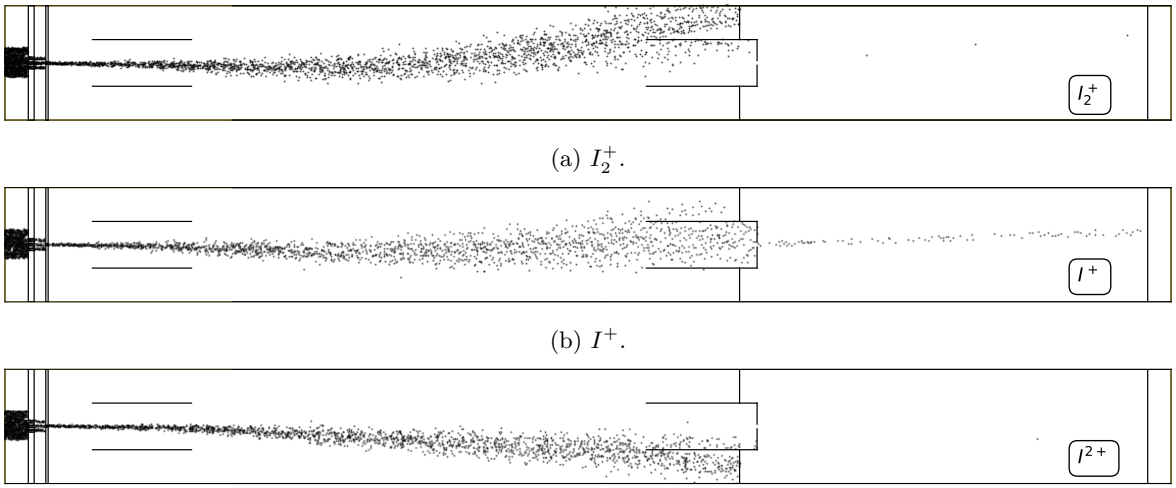

(a) I_2^+.

(b) I^+.

(c) I^{2+}.

Figure 2: Phase space of the simulated ion species. Single charged ions are able to reach the collector (on the right), while molecular ions and double charged ions are deviated by electric and magnetic field respectively.

III. Experimental results

A. Current density and ion energy measurement

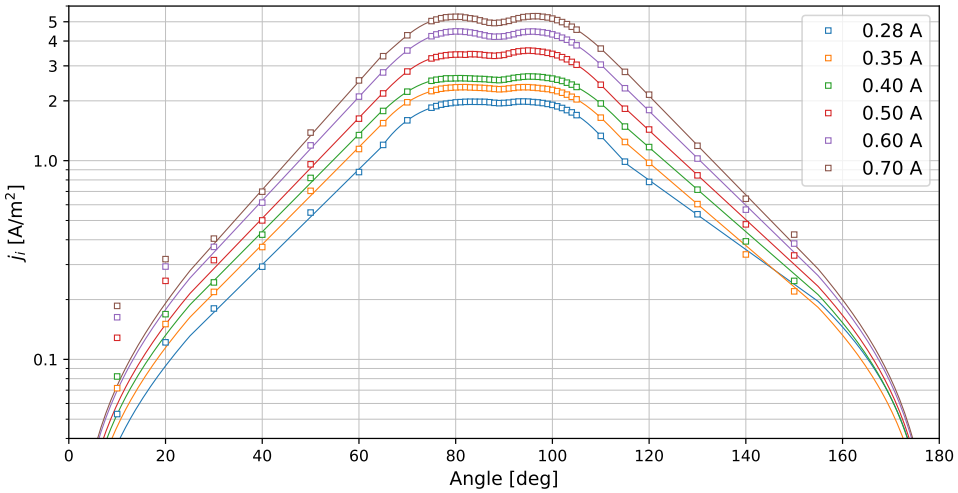

Figure 3: Current density measurements of JPT150's plume. Markers indicate raw data, lines indicate the data fit. All measures were taken at $V_{anode} = 250$ V.

Current density is measured at various discharge current conditions. The results are presented in Fig.3. The presence of a double peak structure at the center of the plume shows good focusing of the ion beam, validating the magnetic field design. In order to extrapolate total beam current and beam divergence, the data was treated to account for the presence of slow charge exchange ions at large angles away from the beam center. Furthermore, secondary electron emission and grid transparency are also taken into account. Integrating over the fitted data over angular span of the measurement provides the beam efficiency and the divergence of the plume. They are presented in Tab.1. The divergence half-angle was taken at 95 % of the total beam current.

Operating point	η_V	η_I	Divergence half angle
250 V - 0.28 A	0.872 ± 0.018	0.755 ± 0.027	55.7°
250 V - 0.35 A	0.864 ± 0.017	0.735 ± 0.021	55.7°
250 V - 0.40 A	0.856 ± 0.017	0.736 ± 0.018	55.7°
250 V - 0.50 A	0.872 ± 0.018	0.749 ± 0.015	54.2°
250 V - 0.60 A	0.872 ± 0.018	0.787 ± 0.013	53.1°
250 V - 0.70 A	0.860 ± 0.017	0.800 ± 0.011	52.1°

Table 1: η_V, η_I, and divergence half angle at different operating points.

Ion energy distribution functions (IEDFs) were measured via the RPA probe and are shown in Fig.4. On-axis RPA measurements are used to measure the voltage efficiency η_V, presented in Tab.1.

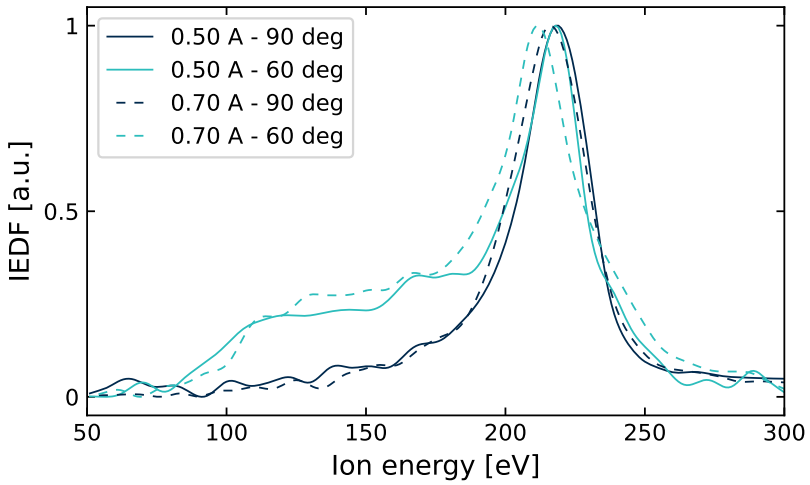

Figure 4: Ion energy distribution function at various discharge current, both on axis (90 deg.) and off-axis (60 deg.). All measures were taken at $V_{anode} = 250$ V.

B. Wien filter results

Preliminary results measured with the Wien filter in the plume of JPT150 are presented at Fig.5. As predicted by PIC simulations, the resolution of the probe is poor, making precise assumptions on the beam composition difficult. The large spread of the peak generated by single charged ions cannot be caused by thruster phenomena, as RPA readings do not show such a large spread of ion energies, and is thus to be attributed to probe resolution.

Fig.5 shows a smaller peak to the left of and partially obscured by the central peak. Assuming that atomic ions are the main population found in the beam and thus the source of the main central population measured, the presence of a smaller peak found at approximately 1.45 times lower Wien filter voltages than that caused by atomic ions indicates a non-negligible presence of ionized molecules I_2^+ in the beam.

Combined operation of RPA and Wien filter is shown in Fig.6. The Wien filter's electric field was set to allow single charged ions to reach its collector. At the same time, the RPA collector's repelling potential was swept. As is visible in Fig.6, the ion flux reaching the Wien filter collector decreases as the RPA repelling bias is increased, and reaches zero when the repelling potential is equal to the anode potential (250 V). It should be noted, however, that the measured trend differs from what is expected of a high-pass filter such as the RPA, with the current dropping almost linearly as the repelling bias is increased. A more concentrated drop is expected given the ion energy distribution functions measured (as shown in Fig.4). PIC simulations have shown that the incoming ions are slowed down by the repelling potential of the RPA and only gradually regain their original velocity after the RPA collector. This allows the cross-drift thermal velocity to affect their trajectories in greater fashion, thus leading to a considerably larger divergence of the ion beam inside

of the Wien filter. Consequently, more ions are lost to the walls of the Wien filter and the flux of ions reaching the its collector is decreased. This makes comparing measures at different RPA repelling potentials difficult, as the changes caused by the increased divergence of the beam are difficult to estimate. In the future, measures will be taken at a constant RPA repelling bias, and the Wien filter will be swept instead.

IV. Conclusion

The current density and ion energy results confirm the performance of JPT150. Basic functions of the combined RPA and $E \times B$ probe are demonstrated, though improvements in the probe's resolution are needed to obtain reliable beam composition data. A second iteration of the probe is being assembled at the time of writing. The new design involves a longer Wien filter section, giving further space to deviate the incoming ions, improving the filter's resolution.

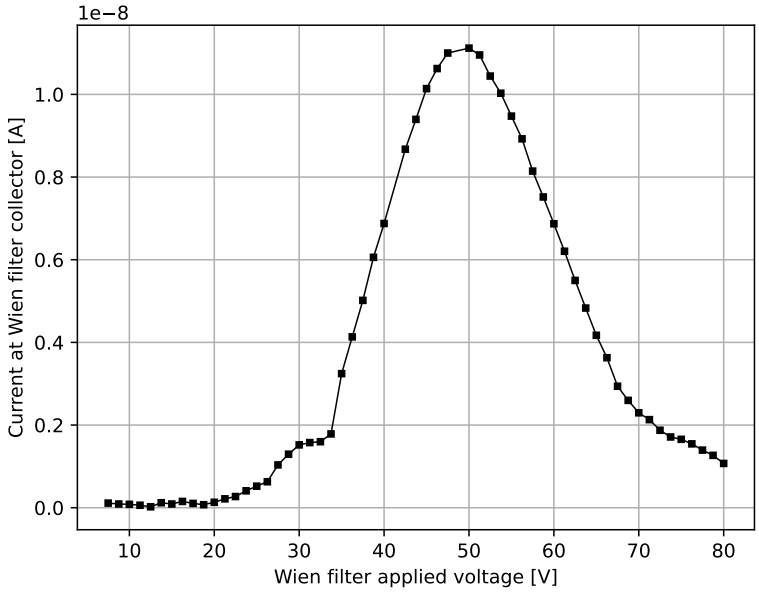

Figure 5: Result of a Wien filter scan. The plume measured is generated by JPT150 operating at $V_{anode} = 250$ V, $I_d = 0.4$ A.

Acknowledgments

Francesco Mattia Bianchi benefits from a CIFRE Ph.D. Funding Grant (No. 2023/0382).

References

[1] Rafalskyi, D., Martínez, J. M., Habl, L., Zorzoli Rossi, E., Proynov, P., Boré, A., Baret, T., Poyet, A., Lafleur, T., Dudin, S., and Aanesland, A., "In-orbit demonstration of an iodine electric propulsion system," *Nature*, Vol. 599, No. 7885, Nov. 2021, pp. 411–415, Number: 7885 Publisher: Nature Publishing Group.

[2] Szabo, J., Pote, B., Paintal, S., Robin, M., Hillier, A., Branam, R. D., and Huffmann, R. E., "Performance Evaluation of an Iodine-Vapor Hall Thruster," *Journal of Propulsion and Power*, Vol. 28, No. 4, July 2012, pp. 848–857.

[3] Szabo, J., Robin, M., Paintal, S., Pote, B., Hruby, V., and Freeman, C., "Iodine Plasma Propulsion Test Results at 1–10 kW," *IEEE Transactions on Plasma Science*, Vol. 43, No. 1, Jan. 2015, pp. 141–148.

[4] Esteves, B., Vicol, R., Laurent, B., Duchemin, O., Tsankov, T. V., Petronio, F., and Chabert, P., "Iodine

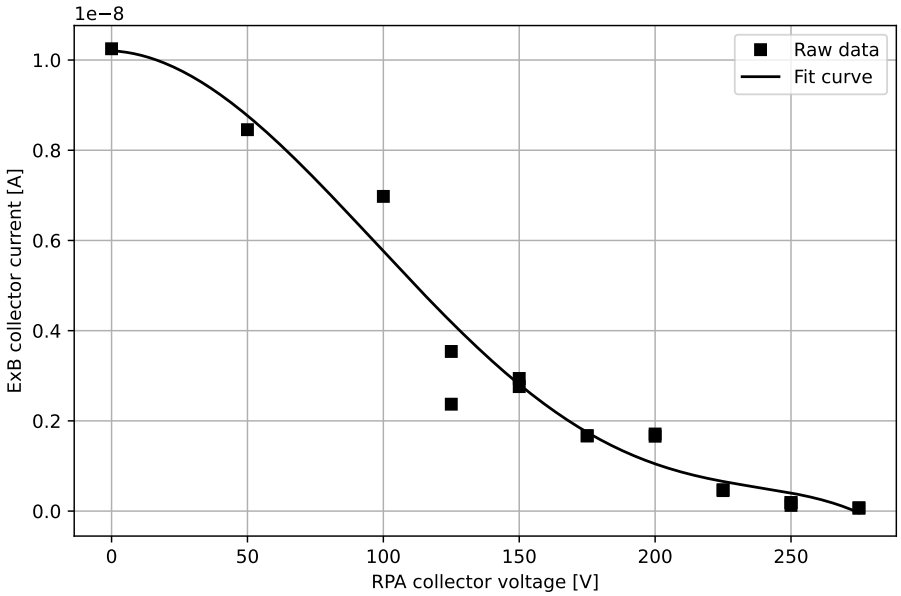

Figure 6: Combined RPA and $E \times B$ operation. $E \times B$ filter set to I^+. Current of $E \times B$ collector is read as repelling potential of RPA collector is swept. JPT150 operating at $V_{anode} = 250$ V, $I_d = 0.4$ A.

(I2) and noble gases (Xe, Kr, Ar) plasma physics for HETs with preliminary characterisation of the PPS® X00 running on these alternative propellants," *International Electric Propulsion Conference, Toulouse, France*, 2024, p. 559.

[5] Vinci, A., Rafalskyi, D., Bhaat, H., Bianchi, F., Dubois, T., and Zorzoli Rossi, E., "Demonstrating low-power iodine-fed Hall thruster propulsion system," May 2025.

[6] Bianchi, F. M., Vinci, A. E., and Garrigues, L., "Global modeling of iodine Hall thruster performance and discharge properties," *Journal of Applied Physics*, Vol. 137, No. 4, Jan. 2025, pp. 043301.

[7] Szabo, J. and Robin, M., "Plasma Species Measurements in the Plume of an Iodine Fueled Hall Thruster," *Journal of Propulsion and Power*, Vol. 30, No. 5, 2014, pp. 1357–1367, Publisher: American Institute of Aeronautics and Astronautics _eprint: https://doi.org/10.2514/1.B35075.

[8] Verboncoeur, J., Langdon, A., and Gladd, N., "An object-oriented electromagnetic PIC code," *Computer Physics Communications*, Vol. 87, No. 1-2, May 1995, pp. 199–211.